



Compressive Strength of FRP-Reinforced and Confined Concrete Columns

Ali Raza¹ · Babar Ali² · Faraz UI Haq³

Received: 1 September 2020 / Accepted: 12 December 2020 / Published online: 18 January 2021
© Shiraz University 2021

Abstract

Nowadays, the practice of fiber-reinforced polymers (FRPs) as an internal reinforcement and external wrapping has been expanded in the construction industry. No theoretical model for estimating the compressive strength (CS) of FRP bars reinforced concrete (RC) columns wrapped with FRP sheets (FRCFS columns) has been found in the literature. The main goal of the current research work is to recommend a new theoretical model for estimating the CS of FRCFS columns. To secure the aims of the present work, the previous research works were employed to construct two different records. The first record consists of 500 sample points of FRP-wrapped concrete specimens, and the second record consists of 269 sample points of FRP bars RC columns. Some initial assessments were carried out on the collected records to select the most suitable forms of the recommended models for FRP-wrapping and CS of FRP bars RC columns. The estimations of these models presented higher accuracy as compared with the previously recommended models. Finally, a new theoretical model was recommended for the CS of FRCFS columns. Then, an extensive parametric study of 216 specimens of FRCFS columns was carried out using the recommended theoretical model.

Keywords Fiber-reinforced polymer · Root mean square error · Axial compressive strength · Columns · Confined concrete

1 Introduction

Nowadays, the use of glass fiber-reinforced polymers (GFRPs) in corrosive environments has become a marvelous interest to evade the corrosion of steel bars (Mohamed et al. 2013; Hassan et al. 2018; Tošić et al. 2018; Hadhood et al.

2019; Van Cao and Pham 2019). In the Canada and USA, the concrete bridge decks are being constructed by using partial or total FRP reinforcement. In spite of this utilization, the Canadian and North American standards did not consider the practice of fiber-reinforced polymers (FRPs) in the concrete piers and compressive members except AASHTO LRFD (2018) that presents guidelines for GFRP-reinforced concrete and CSA S6-19 (2019) that presents useful recommendation for GFRP-reinforced bridge deck slabs and compression members. Therefore, it is necessary for the practical implementation of corrosion resistant FRP bars in the axial concrete members to explore the structural behavior of FRP bars reinforced concrete (RC) columns and to recommend the new theoretical models for the accurate estimations of the behavior of these members.

During the last few decades, the practical applications of GFRP bars have been increased for providing the transverse and longitudinal reinforcements in flexural and compressive members (Mohamed et al. 2014a, b; Mohamed et al. 2016; Bagheri et al. 2019). Various studies explored the compressive behavior of concrete columns having GFRP bars and GFRP ties/spirals as internal reinforcement for resisting the axial compressive loads and flexural moments (Elshamandy

Supplementary information The online version of this article (<https://doi.org/10.1007/s40996-020-00570-y>).

✉ Ali Raza
aliraza@piet.edu.pk
Babar Ali
babar.ali@cuisahiwal.edu.pk
Faraz UI Haq
engrfaraz@uet.edu.pk

- ¹ Department of Civil Engineering, Pakistan Institute of Engineering and Technology, Multan 66000, Pakistan
- ² Department of Civil Engineering, COMSATS University Islamabad Sahiwal Campus, Sahiwal 57000, Pakistan
- ³ Center of Excellence in Water Resources Engineering, University of Engineering and Technology, Lahore 54890, Pakistan

et al. 2018; Dong and Yang 2018; Elchalakani et al. 2019). The investigations are being carried out to determine the reduction factors for the strength of concrete and GFRP bars in axially loaded concrete members by using the concept of steel reinforcements (Tobbi et al. 2012; Zadeh and Nanni 2012; Afifi et al. 2013a, b; Xue et al. 2014). However, an improvement is required in the strength reduction coefficients for GFRP bars in concrete members by using a large experimental record of FRP bars RC members. Some experimental investigations on RC columns reinforced with GFRP bars depicted that by improving the lateral confinement of the concrete core, the ductility and the axial compressive strength (CS) of FRP bars RC columns increase but portraying fewer values of these parameters as compared with steel RC columns (Elchalakani et al. 2017; Elchalakani and Ma 2017; Khorramian et al. 2017; Tabatabaei et al. 2018; Elmessalami et al. 2019; Dadvar et al. 2020; Moshiri et al. 2015; Mostofinejad and Ilia 2014; Mostofinejad and Moshiri 2015; Saljoughian and Mostofinejad 2017; Mostofinejad and Torabian 2016). The theoretical estimations are underestimated, if the axial compressive involvement of GFRP bars is neglected in the axial CS of GFRP-RC compressive members, while including the axial contribution of GFRP bars in the axial CS of columns, a good correlation with the experimental results is obtained (Elchalakani et al. 2017; Elshamandy et al. 2018).

Various investigations are available in the literature that explore the behavior of GFRP-reinforced and confined structural elements using different confinement methods and configurations (Abdelazim et al. 2020a; Abdelazim et al. 2020b; Tabatabaei et al. 2020; Mai et al. 2020; Hasan et al. 2019; Saljoughian et al. 2020; Mai et al. 2018; Hosseini et al. 2020; Lim and Ozbakkaloglu 2014; Naderpour and Mirrashid 2020; Al-Nimry and Neqresh 2019). After performing experiments over the large scale RC columns reinforced with GFRP bars, De Luca et al. (2010) concluded that the design of transverse reinforcement could not be the same for steel and GFRP reinforcement. When a proper lateral confinement is provided to the RC columns reinforced with GFRP bars, the axial compressive contribution of GFRP longitudinal bars is about 5–11% (De Luca et al. 2010; Tobbi et al. 2012; Karim et al. 2016). Tobbi et al. (2012) explored the structural behavior of RC columns reinforced with GFRP bars and portrayed that the lateral GFRP ties provide an effective lateral confinement to the concrete core. When the vertical spacing of GFRP ties was reduced from 120 to 80 mm, an improvement of 20% occurred in the CS of RC columns reinforced with GFRP bars. After studying the structural behavior of GFRP and steel RC columns (hybrid columns), Pantelides et al. (2013) concluded that for securing the same structural performance as represented by steel RC columns, the higher reinforcement ratios for transverse and longitudinal bars should be provided in RC columns reinforced with

GFRP bars. Afifi et al. (Afifi et al. 2013a, b; Afifi et al. 2015; Afifi et al. 2014) examined the performance of full-scale carbon fiber-reinforced polymer (CFRP) bars RC columns and recommended the new models for estimating the axial CS of such members. Furthermore, they concluded that the CFRP bars can contribute up to 10% in the axial CS of CFRP bars RC columns. Several studies recommended the models for predicting the axial CS of FRP-wrapped concrete members (Rasouli et al. 2020; Raza et al. 2020a, 2020b, 2020c, 2020d; Raza and Rafique 2020), but none of them suggested the theoretical model for capturing the compressive capacity of FRP-wrapped axially loaded concrete members internally reinforced with FRP bars.

The FRP bars present lower performance in compression. The deficiency of FRP bars in the concrete compression members can be resolved by increasing the lateral confining pressure of compression members i.e., by using strengthening techniques. The strengthening can be efficiently done using FRP sheets because they have high tensile strength which is the major property of the strengthening materials. Furthermore, to overcome the brittle behavior of FRP-reinforced concrete compression members, it is the best way to laterally strengthen them by using CFRP wraps in improving their axial compressive strength, ductility, axial stiffness, and failure behavior. The present investigation aims to accurately predict the axial CS of FRP bars RC columns wrapped with FRP sheets (FRCFS columns). To secure the aim of the present work, two different records from the previous investigations were constructed containing large sample points of FRP-reinforced axially loaded concrete members and FRP-wrapped axially loaded concrete members. Assessment of the records was performed using the previously recommended strength models for FRP-reinforced axially loaded concrete columns and FRP-wrapped axially loaded concrete members. First, a new model for the lateral FRP-wrapping effect was recommended, and then, an equation was suggested for the CS of FRCFS columns. Additionally, a comprehensive parametric study was carried out using the recommended theoretical model for FRCFS columns to inspect the influence of various parameters of FRCFS columns on their axial CS. The recommended model for the axial CS of FRCFS columns will be useful for the design of FRCFS columns.

2 Development of Databases

Two experimental records were constructed in the present study from which one record consisted of the 500 sample points of FRP-wrapped concrete members, and the second record consisted of the 269 sample points of FRP RC members (provided in the supplementary data Table A). The assessment of the record based on

the previous strength models portrayed that some of the sample points were not prophesied by the existing models. Consequently, those sample points were deleted to evade the saturation of the RMSE statistical index. The sample points giving the error of more than 50% were counted to 50 values. The assessment of the strength models was performed using 500 sample points of FRP-wrapped concrete members using two different statistical indices i.e., R^2 and RMSE. The statistical details of 500 FRP-wrapped members are reported in Table 1.

The second record consisted of the sample points of FRP RC columns. The statistical details of the second record have been reported in Table 2. The transverse wrapping was provided by using either steel ties or FRP ties. One hundred and twenty-four columns were having rectangular dimensions, and 145 columns having a circular dimension in the cross section. GFRP spiral-wrapped columns were 110, GFRP hoop-wrapped columns were 100, steel spiral-wrapped columns were 18, steel hoop-wrapped columns were 33, and CFRP spiral-wrapped columns were 8 in total. All the geometric and material details including width of columns (W), breadth of columns (B), diameter of circular columns (D), the CS of concrete (f'_{co}), the elastic modulus of FRP (E_f), the tensile strength of FRP (f_u), transverse reinforcement ratio (ρ_t), the ultimate strain of FRP (ϵ_u), FRP bars ratio (ρ_l), and axial CS of columns (P_n) were provided in the constructed record.

where nt is the thickness of FRP sheets, H is the height of member, f'_{cc} is the maximum CS of wrapped concrete, ϵ_{co} is the maximum compressive strain of unwrapped concrete, ϵ_{cc} is the maximum compressive strain of wrapped concrete.

3 Assessment of Physical Models

3.1 Confinement Effect

First, a strength model for FRP-wrapping was anticipated. Some of the practical parameters such as wrapping stress (f_l), wrapping stiffness ratio (ρ_k), hoop rupture strain of fibers ($\epsilon_{h, rup}$), and strain ratio (ρ_ϵ) are communal for all the previous strength models. The expressions for ρ_k and ρ_ϵ were reported by (Teng et al. 2009) as reported by Eq. (1) and Eq. (2).

$$\rho_\epsilon = \frac{\epsilon_{h, rup}}{\epsilon_{co}} \tag{1}$$

$$\rho_k = \frac{2E_f t}{\left(\frac{f'_{co}}{\epsilon_{co}}\right) D} \tag{2}$$

In this relationship, ' t ' is the thickness of FRP sheets, E_f is Young's modulus of FRP sheets in the transverse direction, and ϵ_{co} is the compressive strain of unwrapped concrete. Figure 1 represents the wrapping stresses due to FRP sheets with a hoop diameter D .

The expression for the maximum wrapping stress (f_l) can be presented in terms of the properties of FRP sheets and concrete specimen as follows (Sadeghian and Fam 2015):

$$f_l = \rho_\epsilon \rho_k f'_{co} = \frac{2E_f \epsilon_{h, rup} t}{D} \tag{3}$$

The hoop rupture strain ($\epsilon_{h, rup}$) due to the transverse wrapping can be expressed in terms of the strain of FRP sheets and concrete strength as represented by Eq. (4) (Lim

Table 1 Statistical details of the first record for FRP-wrapped specimens (SD represents the standard deviation, and COV represents the coefficient of variation)

Parameter	D (mm)	E_f (GPa)	nt (mm)	H (mm)	f'_{co} (MPa)	f'_{cc} (MPa)	ϵ_{co} (%)	ϵ_{cc} (%)
Minimum values	51	10	0.09	102	12.41	18.50	0.17	0.47
Maximum value	406	612	5.90	812	188.2	302.2	1.53	4.62
Average value	153.85	164	0.95	307.93	42.28	75.46	0.27	1.63
SD	45.47	118	1.12	90.92	22.97	32.56	0.16	0.83
COV	0.30	0.73	1.18	0.30	0.55	0.44	0.60	0.51

Table 2 Statistical details of the second record for FRP-reinforced specimens

Parameter	B (mm)	W (mm)	D (mm)	A_g (mm ²)	f'_{co} (MPa)	f_u (MPa)	E_f (GPa)	ϵ_u (%)	ρ_l (%)	A_f (mm ²)	ρ_t (%)	P_n (kN)
Minimum	150	150	150	17,662	20.0	406	23.4	0.97	0.55	212	0.01	114
Maximum	610	610	305	372,100	70.2	1680	141	2.42	5.3	4051	5.3	15,235
Average	249	272	258	66,289	36.2	1010	56.7	1.78	2.09	1214	1.38	1814
SD	114	114	54	53,039	12.6	339	25.1	0.39	1.06	764	1.06	1877
COV	0.46	0.43	0.21	0.81	0.35	0.34	0.45	0.22	0.51	0.63	0.77	1.04

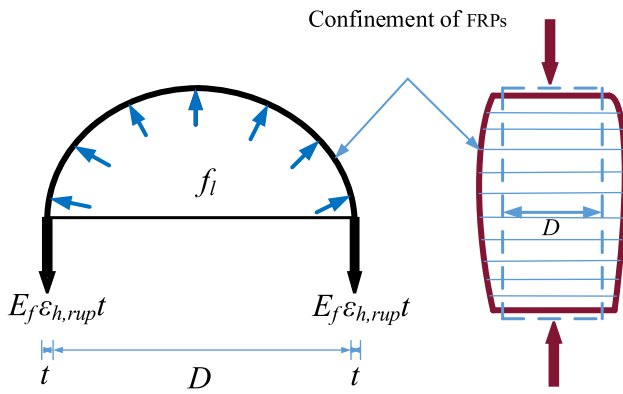


Fig. 1 Wrapping mechanism of FRP sheets

et al. 2016). This relationship was derived using the genetic programming formulation method.

$$\varepsilon_{h, rup} = \frac{\varepsilon_f}{f_{co}^{0.125}} \quad (4)$$

where ε_f represents the maximum tensile strain of FRP sheets.

3.2 Previous Models

Table 3 reports the various strength models anticipated in the previous research for determining the wrapping mechanism of FRP sheets. These models have wide applications due to their acceptance in implementation.

In the present research, the models were recommended by minimizing the percentage errors i.e., sum of the square errors (*SSE*), coefficient of determination (R^2), and root mean squared error (*RMSE*) between the measurements and estimations of previous theoretical models using the curve fitting method. All the strength models as presented in Table 3 were assessed by using the developed record of FRP-wrapped members. The statistical indices (R^2 and *RMSE*) are reported by the Eq. (5) and Eq. (6), respectively.

$$RMSE(x, y) = \sqrt{\frac{\sum (x - y)^2}{n}} \quad (5)$$

Table 3 Previous strength models of FRP wrapped concrete specimens

Strength model	The relationship for strength model
Teng et al. (2009) model	$\frac{f'_{sc}}{f'_{co}} = 1 + 3.5(\rho_k - 0.01)\rho_\varepsilon$
Karbhari and Gao (1997) model	$\frac{f'_{sc}}{f'_{co}} = 1 + 2.1\left(\frac{f_l}{f'_{co}}\right)^{0.87}$
Saafi et al. (1999) model	$\frac{f'_{sc}}{f'_{co}} = 1 + 2.2\left(\frac{f_l}{f'_{co}}\right)^{0.84}$
Matthys et al. (2005) model	$\frac{f'_{sc}}{f'_{co}} = 1 + 2.3\left(\frac{f_l}{f'_{co}}\right)^{0.85}$
Fardis and Khalili (1982) model	$\frac{f'_{sc}}{f'_{co}} = 1 + 3.7\left(\frac{f_l}{f'_{co}}\right)^{0.86}$
Richart et al. (1929) model	$\frac{f'_{sc}}{f'_{co}} = 1 + 4.1\frac{f_l}{f'_{co}}$
Newman and Newman (1971) model	$\frac{f'_{sc}}{f'_{co}} = 1 + 3.7\left(\frac{f_l}{f'_{co}}\right)^2$
Mander et al. (1988) model	$\frac{f'_{sc}}{f'_{co}} = 2.254\sqrt{1 + 7.94\frac{f_l}{f'_{co}} - 2\frac{f_l}{f'_{co}}} - 1.254$
Lam and Teng (2003) model	$\frac{f'_{sc}}{f'_{co}} = 1 + 3.3\frac{f_l}{f'_{co}}$
Toutanji (1999) model	$\frac{f'_{sc}}{f'_{co}} = 1 + 3.5\left(\frac{f_l}{f'_{co}}\right)^{0.85}$
Samaan et al. (1998) model	$f'_{cc} = f'_{co} + 6.0f_l^{0.70}$ where $f_o = 0.872f'_{co} + 0.371f_l + 6.258$ and $E_2 = 245.61f'_{co}{}^{0.2} + 1.3456\frac{E_f t}{D}$
Miyauchi et al. (1997) model	$\frac{f'_{sc}}{f'_{co}} = 1 + 3.485\frac{f_l}{f'_{co}}$

$$R^2(x, y) = \left(\frac{n(\sum xy) - (\sum x)(\sum y)}{\sqrt{[n \sum x^2 - (\sum x)^2][n \sum y^2 - (\sum y)^2]}} \right)^2 \quad (6)$$

where ‘ x ’ is the experimentally measured strength and ‘ y ’ is the theoretically estimated strength, and ‘ n ’ is the number of data. The value of R^2 can vary from 0 to 1. 1 portrays a perfect connection and the best fit while 0 portrays there is no correlation between the theoretical estimations and experimental measurements. Correspondingly, the lesser value of RMSE (close to 0) indicates the good performance of the recommended models and higher value indicates a larger deviation from the experimental results. The sum of squared errors (SSE) was measured by considering the differences between the experimental and theoretical measurements. A lesser value of SSE shows a good correlation with the experimental results. The performance of the aforementioned strength equations with statistical indices R^2 and RMSE is reported in Fig. 2.

3.3 Proposed Strength Model for Confinement

The general form of the suggested model was nominated after the assessment of previous models over the developed record. The Lam and Teng (Lam et al. 2003) model which was implemented by ACI 440.2R-02 (Bakis et al. 2002) with minor alterations show a close correlation with the experimental results with $R^2 = 0.90$ and $RMSE = 0.26$, but the model recommended by Toutanji (1999) portrayed a good behavior with $R^2 = 0.90$ and $RMSE = 0.23$. Thus, the form of the anticipated axial CS model was kept the same as that of the Toutanji (1999) model. The Mander et al. (1988) model which was primarily implemented by ACI 440.2R-02 (2002) presented the RMSE index of 0.22, but its performance for the value of R^2 is not good enough as compared with that given by other models. After evaluating all the models, the final form of the suggested nonlinear model was reported by Eq. (7).

$$\frac{f'_{cc}}{f'_{co}} = 1 + k \left(\frac{f_l}{f'_{co}} \right)^n \quad (7)$$

where k and n are the coefficients that have been calculated by using general regression analysis. The curve fitting method over the developed record reported the values of coefficients k and n as 3 and 0.73, respectively.

$$\frac{f'_{cc}}{f'_{co}} = 1 + 3 \left(\frac{f_l}{f'_{co}} \right)^{0.73} \quad (8)$$

The relationship for the axial CS of FRP-wrapped members can be rewritten as:

$$f'_{cc} = f'_{co} + 3f'_{co}{}^{0.27} \left(\frac{2E_f \epsilon_{h, \text{rup}} t}{D} \right)^{0.73} \quad (9)$$

Figure 3 reports the results of the performance evaluation of the suggested strength model over 500 sample points. It can be observed that the suggested model depicted higher accuracy than the previous strength equations with the statistical indices $R^2 = 0.91$ and $RMSE = 0.18$. Therefore, the currently suggested model has captured the lateral confinement effect provided by the FRP sheets precisely.

Figure 4 reports the distribution of the ratios of FRP-wrapped concrete strength to unwrapped concrete strength of test measurements and theoretical estimates over the developed experimental record and the normal distribution of FRP-wrapped concrete strength to unwrapped concrete strength ratio of the developed experimental record is reported in Fig. 5. There were 251 values of the ratios of FRP-wrapped concrete strength to unwrap the concrete strength of test measurements and empirical values in the range of 0–1.5. Karbhari and Gao (1997) model provided 258 values being the highest, while all other models reported fewer values in the range of 0–1.5. Although the Karbhari and Gao (1997) model reported the good distribution of estimations, it did not present good performance based on the statistical indices. The suggested model reported 203 sample points in the range of 1.51–3.00, and 46 sample points in the range of 3.01–6.00 being the most accurate one. The Toutanji (1999) model reported a better performance for the normal distribution having a deviation of 1.5% from unity. The recommended model portrayed a percent deviation of 1% from unity solidly validating its accuracy. Conclusively, the recommended strength model is more accurate than the previous models.

3.4 Proposed Strength Model for FRCFS Columns

Twelve models taken from the literature were assessed over the second record for the axial CS of FRP bars RC columns to choose a form for the newly recommended model. All the previous models for the CS of FRP RC specimens are reported in Table 4. These models were assessed based on the second record using R^2 , RMSE, and SSE to minimize the error of estimations. The parameter R^2 is the most vital for the assessment of the estimations; therefore, this parameter was employed in the present study for the selection of the better form of the model.

The assessments of all the recommended models in the literature have appeared in Fig. 6. The Afifi et al. (2013a, b) model spoke to the most noteworthy estimation of $R^2 = 0.711$. As the estimation of R^2 builds, the precision of expectation increments. At the point when the estimation of R^2 is 1.0, it speaks to an ideal connection between the

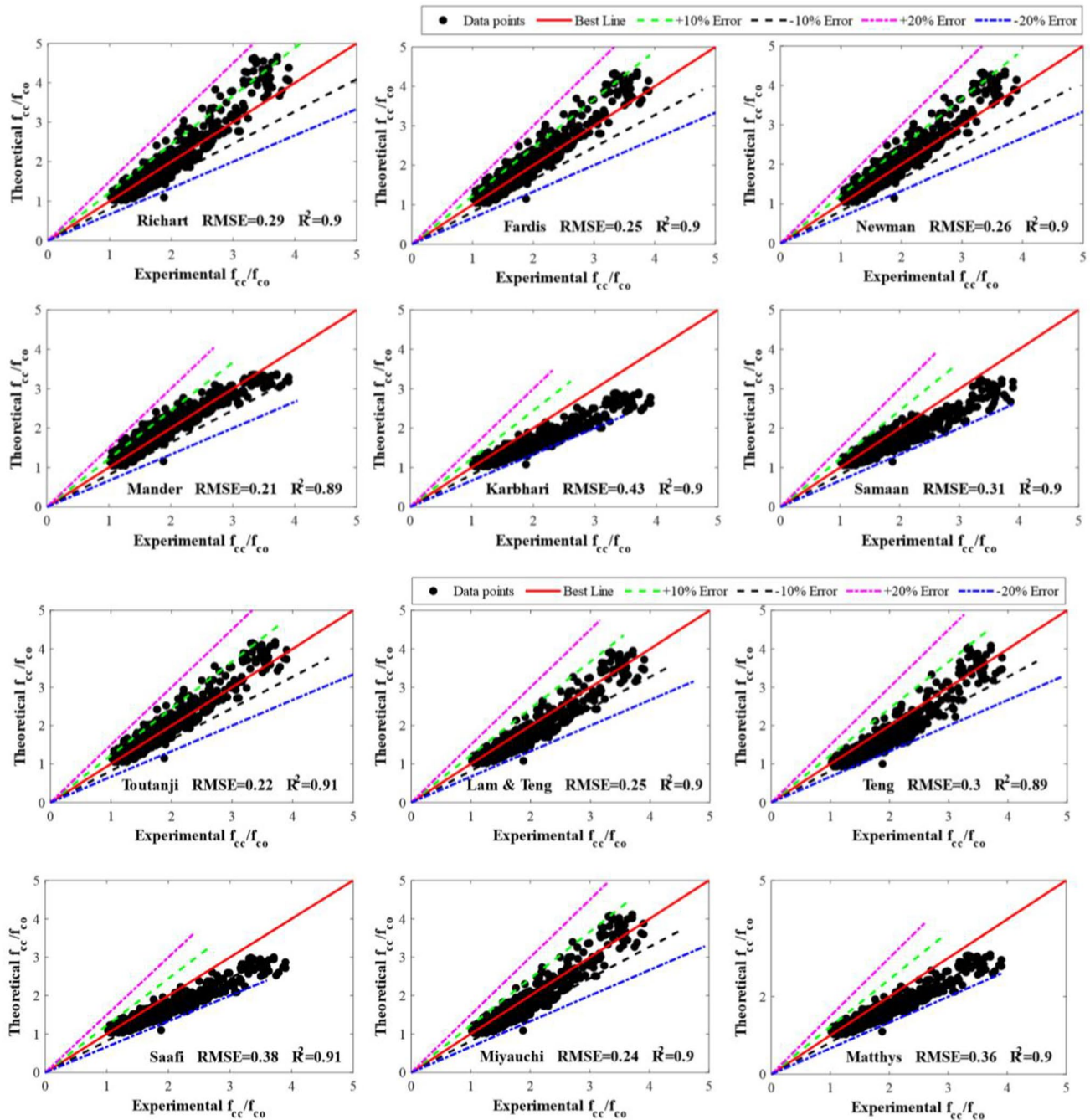


Fig. 2 Performance of strength models on the first record

testing measurement and anticipated consequences of axial CS. Subsequently, the overall type of the recommended limit model was viewed as that of the model recommended by Afifi et al. (2013a, b). Then again, the commitment of FRP reinforcement in the maximum axial CS of GFRP-RC columns was included because of their elasticity and cross-sectional zone by applying a decrease coefficient.

The form of the recommended model is reported by Eq. (10).

$$P_n = \alpha_1 (A_g - A_{FRP}) f'_{co} + \alpha_2 f_{FRP} A_{FRP} \quad (10)$$

where α_1 and α_2 are the reduction coefficients for the axial CS of RC columns reinforced with GFRP bars indicating the reduction in the concrete core and longitudinal FRP bars, respectively. A_g is the area of cross section, A_{FRP} is the area of FRP longitudinal reinforcement, and f_{FRP} is the ultimate tensile strength of longitudinal reinforcement. The values of α_1 and α_2 were measured by using the curve fitting method

Fig. 3 Performance of the suggested strength model on the first record

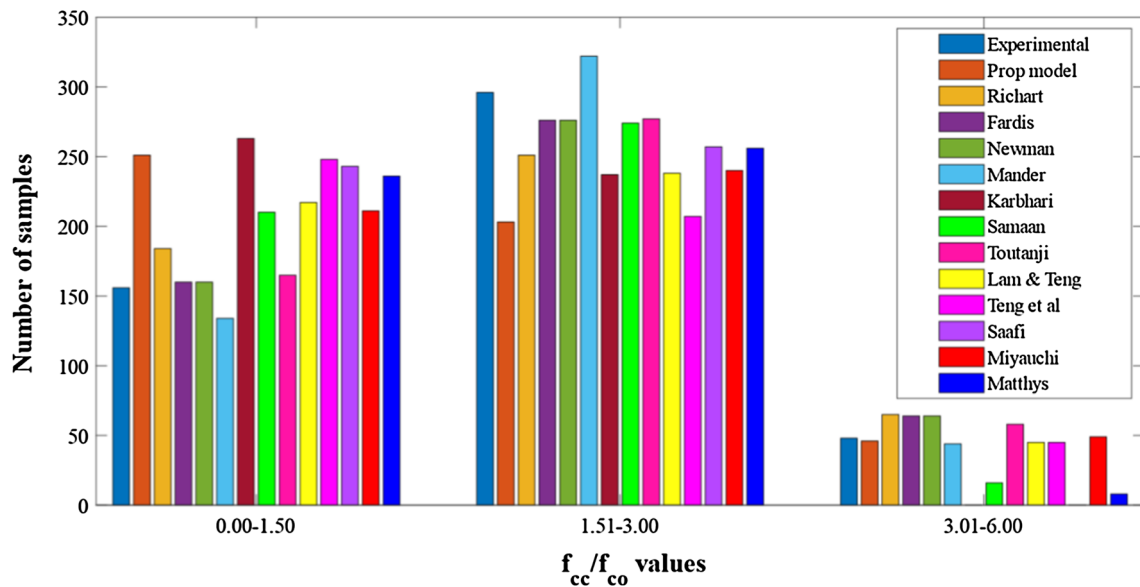
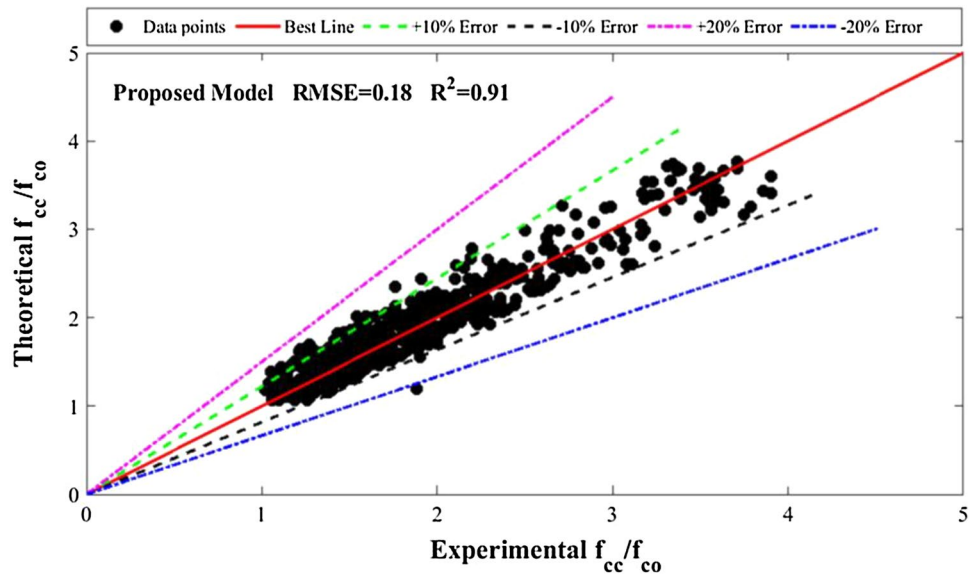


Fig. 4 Distribution of f'_{cc}/f'_{co} for FRP-wrapped specimens based on estimations of various strength models

over the constructed record to secure the best fit. The expression for α_1 can be represented by $\alpha_1 = 0.85 - \beta f'_{co}$ following CSA S806-12 (2012), where β is another constant. Hence, Eq. (10) can be rewritten as:

$$P_n = (0.85 - \beta f'_{co})(A_g - A_{FRP})f'_{co} + \alpha_2 f_{FRP} A_{FRP} \quad (11)$$

The determined values of the coefficients α_2 and β from the curve fitting method were 0.0208 and 0.0029, respectively. After inserting the values of these coefficients, Eq. (11) could be transformed into Eq. (12).

$$P_n = (0.85 - 0.0029f'_{co})(A_g - A_{FRP})f'_{co} + 0.0208f_{FRP}A_{FRP} \quad (12)$$

Equation (12) reports the final model recommended in the present work for apprehending the axial CS of FRCFS columns with sufficient accuracy being superior to the recommended models in the literature. The reduction coefficients (α_1) for the concrete core should be greater than 0.65 i.e. $\alpha_1 = 0.85 - 0.0029f'_{co} \geq 0.65$. The recommended model portrayed the best performance with $R^2 = 0.73$ being the highest among all the previous models as reported in Fig. 7.

Fig. 5 Normal distribution of $(f'_{cc}/f'_{co,exp})/(f'_{cc}/f'_{co,pred})$ for FRP-wrapped specimens based on estimations of various strength models

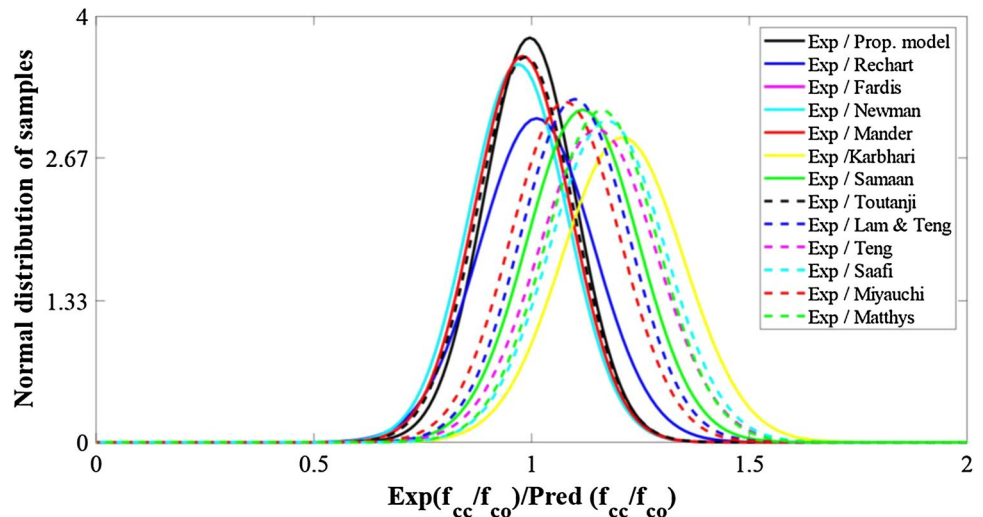


Table 4 Different axial CS models of FRP reinforced columns for assessment

Research/code	Expression for axial strength
Canadian Standards Association CSA S806-12 (2012a, b)	$P_n = \alpha_1 f'_c (A_g - A_{FRP}); \alpha_1 = 0.85 - 0.0015 f'_c \geq 0.67$
Afifi et al. (2013a, b)	$P_n = 0.85 f'_c (A_g - A_{FRP}) + \alpha_g f_{FRP} A_{FRP}; \alpha_g = 0.35$
ACI Committee ACI-318–11 (2011a, b)	$P_n = 0.85 f'_c (A_g - A_s)$
ACI 318–08 (2008)	$P_n = 0.85 f'_c (A_g - A_s) + f_y A_s$
CSA S806-02 (2002)	$P_n = 0.85 f'_c (A_g - A_{FRP})$
AS-3600 (2018)	$P_n = 0.85 f'_c (A_g - A_{FRP}) + 0.0025 E_{FRP} A_{FRP}$
Mohamed et al. (2014a, b)	$P_n = 0.90 f'_c (A_g - A_{FRP}) + \epsilon_{fg} E_{FRP} A_{FRP}; \epsilon_{fg} = 0.002$
Tobbi et al. (2014)	$P_n = 0.85 f'_c (A_g - A_{FRP}) + \epsilon_{co} E_{FRP} A_{FRP}; \epsilon_{co} = 0.003$
Samani and Attard (2012)	$P_n = 0.85 f'_c (A_g - A_{FRP}) + 0.0025 E_{FRP} A_{FRP}$
Hadhood et al. (2016)	$P_n = \alpha_1 f'_c (A_g - A_{FRP}) + 0.0035 E_{FRP} A_{FRP}; \alpha_1 = 0.85 - 0.0015 f'_c$
Khan et al. (2016)	$P_n = 0.85 f'_{cc} (A_g - A_{GFRP}) + \alpha f_{GFRP} A_{GFRP}; \alpha = 0.61$
Mohamed et al. (2014a, b)	$P_n = 0.85 f'_c (A_g - A_{FRP}) + \epsilon_p E_{FRP} A_{FRP}; \epsilon_p = 0.002$

The circulation of the past testing measurements and anticipated axial CSs of GFRP bars RC members is introduced in Fig. 8. There were 119 exploratory estimations of axial CSs in the scope of 1000 to 0 kN in the built record. The recommended model gave 100 sample points in this range which substantiates its boss execution over different models. So also, the test and anticipated sample points were 134 and 175 in the scope of 4000 to 1001 kN, 22 and 2 in the scope of 10,000 to 4001 kN, 4 and 2 in the range 16,000 to 10,001 kN, individually. These sample points speak to that the recommended model caught the axial CS of GFRP bars RC sections well.

The normal dispersion of testing measurements to anticipated estimations of axial CSs of GFRP-reinforced specimens from the developed record for all the already and at present recommended models is introduced in Fig. 9. The recommended model presented good performance for the mean standardized estimations of proportions of testing

measurements to anticipated values with an eccentricity of just 4% from solidarity. The most extreme eccentricity of 41% was watched for ACI-318–08. This may be associated with the cause that the model suggested by ACI-318–08 was given for the steel bars, while this model is utilized in current work for only a relative investigation. Furthermore, the percent eccentricities for the equations reported by Afifi et al. (2013a, b), Khan et al. (2016), CSA S806-12 (2012) were 21%, 30%, and 4.5%, respectively.

By considering the wrapping mechanism in the present study, the unwrapped strength of concrete was assumed to be equal to the FRP-wrapped strength of concrete. Therefore, in Eq. (12) f'_{co} was transformed to f'_{cc} as reported by Eq. (13). This is the suggested model for calculating the CS of FRCFS columns.

$$P_n = (0.85 - 0.0029 f'_{co}) (A_g - A_{FRP}) f'_{cc} + 0.0208 f_{FRP} A_{FRP} \tag{13}$$

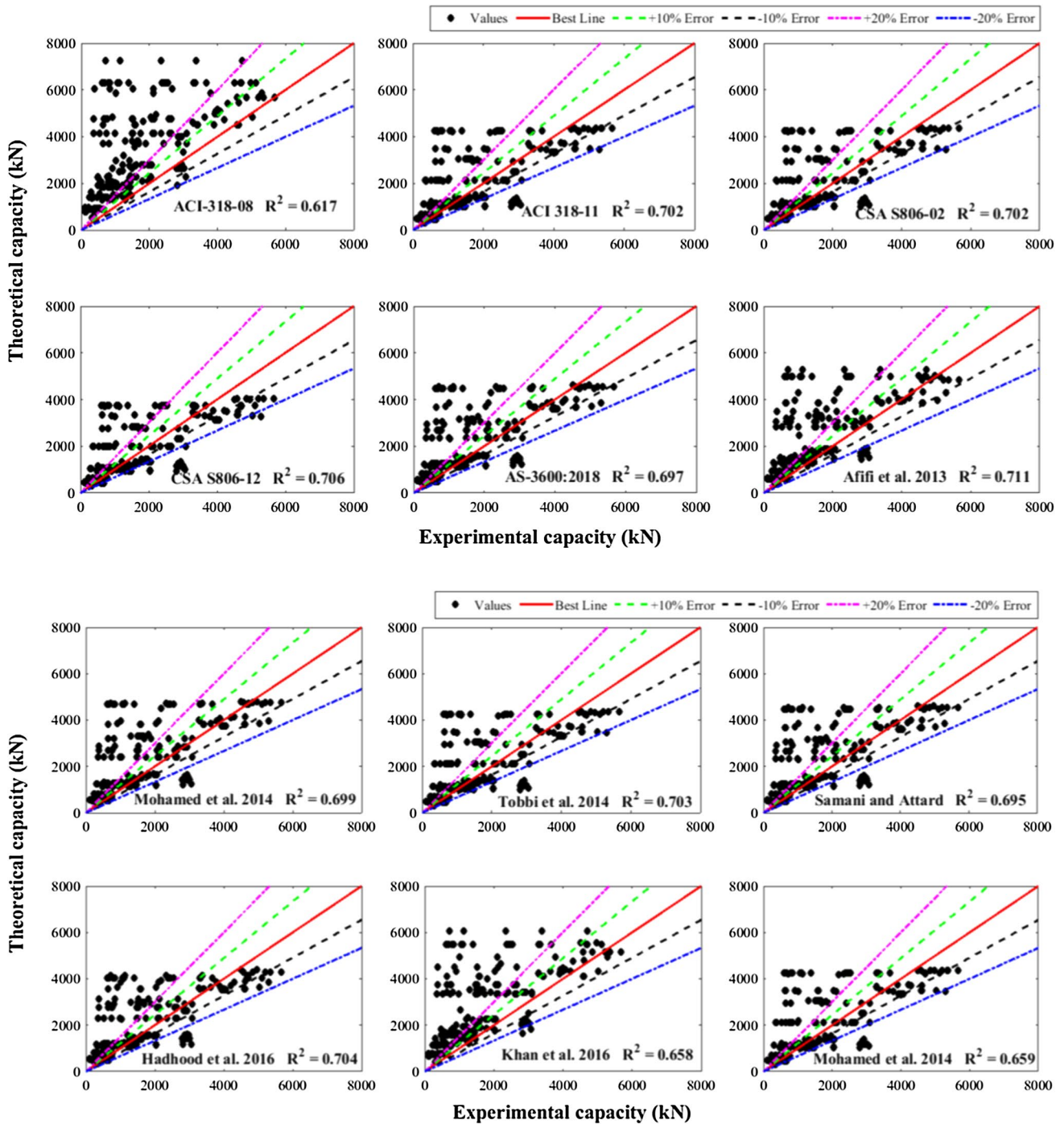


Fig. 6 Performance of CS models for FRP-reinforced columns

4 Parametric Study

The recommended model for catching the CS of FRCFS columns (introduced by Eq. (13)) was utilized to complete a broad parametric examination. Different boundaries of FRCFS columns, for example, the thickness of GFRP sheet (t_{GFRP}), unwrapped concrete strength (f'_{co}),

GFRP longitudinal bars proportion and the measurement of diameter (D) were evaluated to research their effect on the CS of FRCFS columns by testing 216 examples. Different values for FRP bars proportion were 2.2, 2.0, 1.8, 1.6, 1.4, and 1.2%; for f'_{co} , the different values were 65, 55, 45, 35, 25, and 15 MPa; for t_{GFRP} , the different values were 3.0, 2.5, 2.0, 1.5, 1.0, and 0.5 mm; and for D , the different

Fig. 7 Performance of the newly recommended model

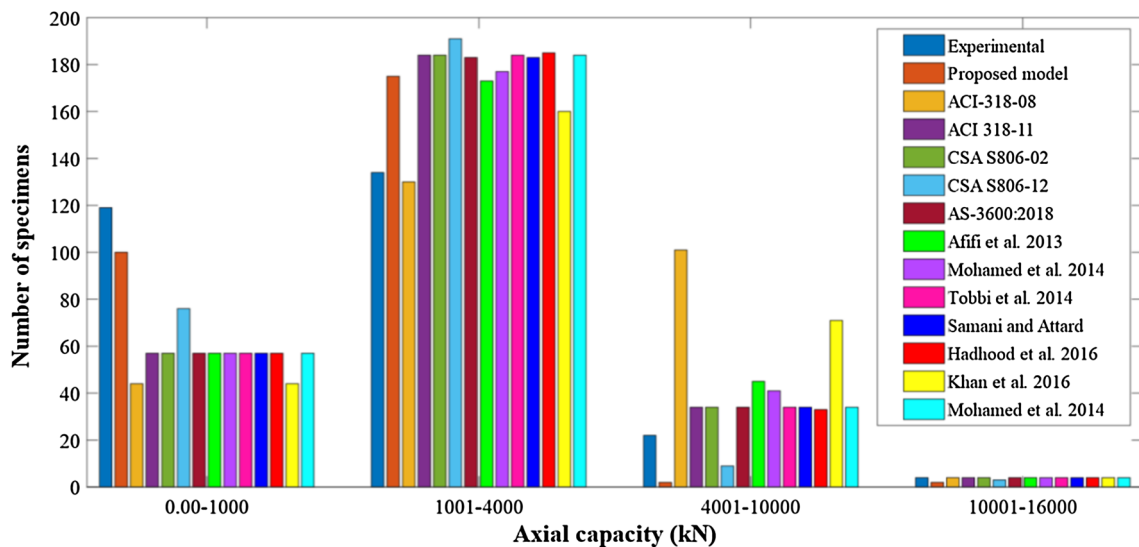
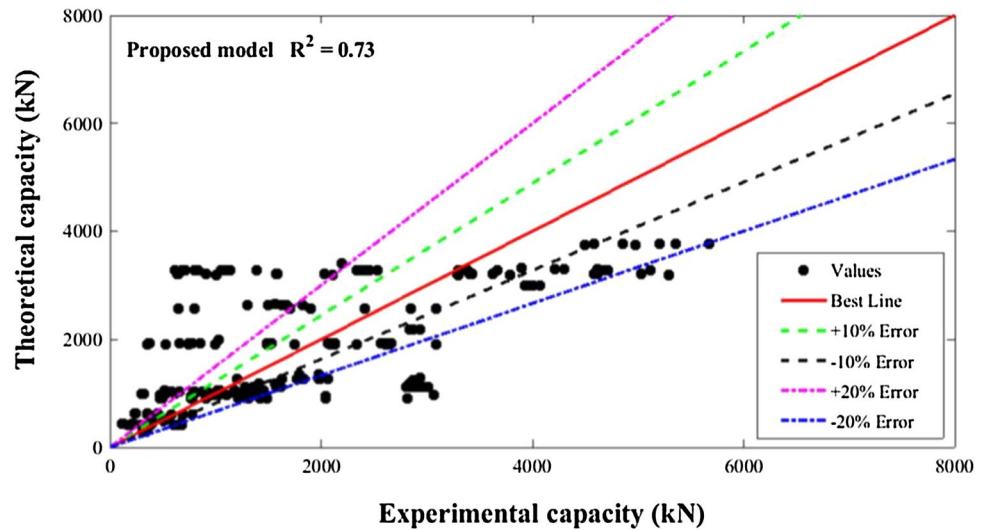


Fig. 8 Distribution of the estimations of various strength models on the constructed record

values were 350, 300, 250, 200, 150, and 100 mm. The steady values for the CS of concrete, FRP longitudinal bars proportion, GFRP sheet thickness, and width of the columns were 25 MPa, 1.8%, 2.0 mm, and 200 mm, individually. All the specimens were 800 mm in tallness. The Young’s modulus of the GFRP sheet, the yielding quality of the GFRP sheet, and the maximum strength of GFRP bars were taken by (Hadi et al. 2016).

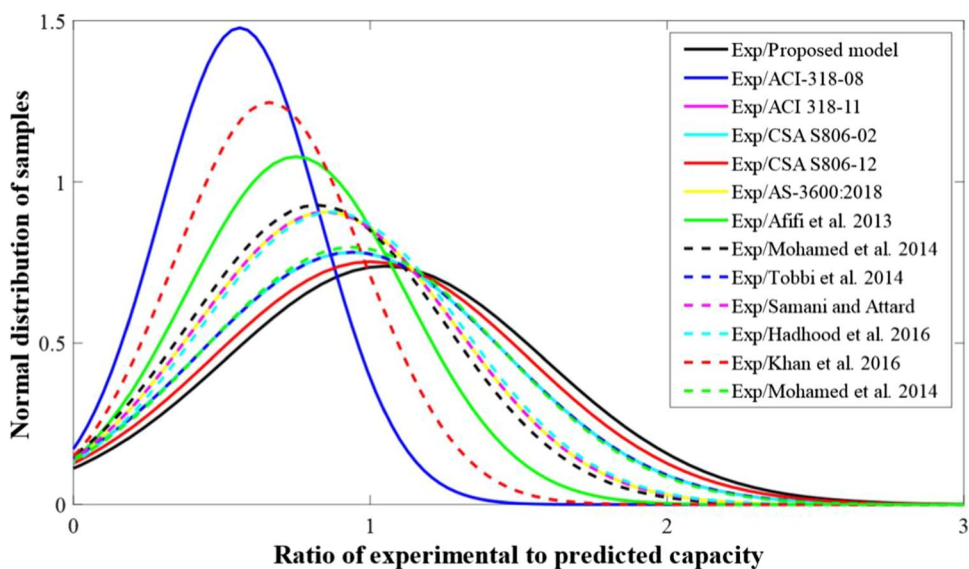
4.1 GFRP Longitudinal Reinforcement Ratio (ρ_l)

The consequence of ρ_l was assessed by using six different values i.e., 2.2%, 2.0%, 1.8%, 1.6%, 1.4%, and 1.2%. By enhancing the ρ_l from a minimum value of 1.2% to a maximum value of 2.2% along with enhancement of f'_{co} from 15

to 65 MPa by keeping the contact values of $t_{GFRP}=2$ mm and $D=200$ mm, an improvement of 212.5% occurred in the CS of FRCFS columns. Correspondingly, by enhancing the ρ_l from a minimum value of 1.2% to a maximum value of 2.2% along with enhancement of t_{GFRP} from 0.5 to 3 mm by keeping the contact values of $f'_{co}=25$ MPa and $D=200$ mm, an improvement of 64% occurred in the CS of FRCFS columns.

Moreover, an improvement of 1282.7% occurred in the CS by enhancing the ρ_l from a minimum value of 1.2% to a maximum value of 2.2% along with enhancement of D from 100 to 350 mm by keeping the contact values of $f'_{co}=25$ MPa and $t_{GFRP}=2$ mm. Effect of ρ_l on the CS of FRCFS columns with the enhancement of f'_{co} , t_{GFRP} and D is separately reported in 3-D Fig. 10(a, b, c). It was observed that the influence of increasing ρ_l along with the improvement in

Fig. 9 Normal distribution of the testing results to theoretical estimations of various strength models on the constructed record



diameter was more leading with the percentage increase of 1282.7% in the CS.

4.2 Unwrapped Concrete Strength (f'_{co})

The consequence of f'_{co} on the CS is reported in Fig. 10 (a, d, e). By enhancing the f'_{co} from a minimum value of 15 MPa to a maximum value of 65 MPa along with enhancement of ρ_l from 1.2 to 2.2% by keeping the contact values of

$t_{GFRP}=2$ mm and $D=200$ mm, an improvement of 212.5% occurred in the CS of FRCFS columns. Correspondingly, by enhancing the f'_{co} from a minimum value of 15 MPa to a maximum value of 65 MPa along with enhancement of t_{GFRP} from 0.5 to 3 mm by keeping the contact values of $\rho_l=1.8\%$ and $D=200$ mm, an improvement of 222.2% occurred in the CS of FRCFS columns. Similarly, the result of the increase in f'_{co} was 1051.7% improvement in the CS FRCFS columns due to an enhancement in the diameter of FRCFS columns.

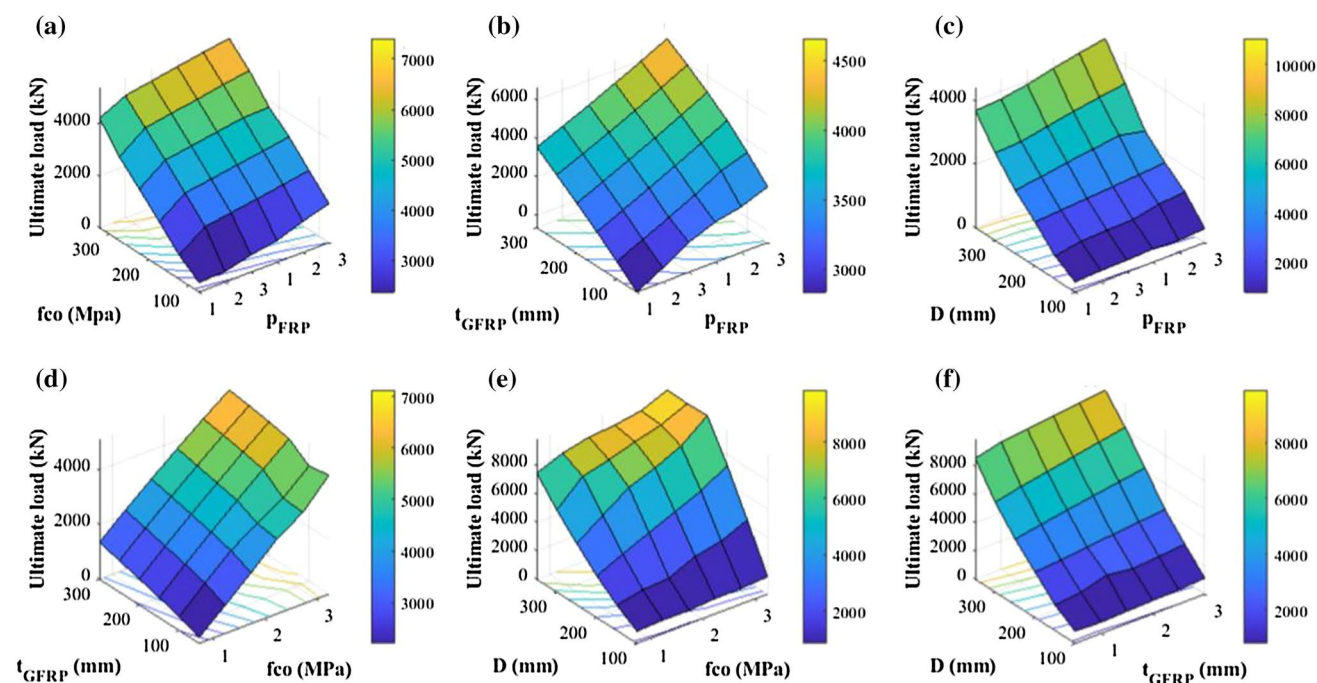


Fig. 10 Effect of longitudinal reinforcement ratio, the CS of concrete, the thickness of GFRP sheet, and the diameter of FRCFS columns on the maximum CS of FRCFS columns

4.3 GFRP Sheet Thickness (t_{GFRP})

The consequence of t_{GFRP} was assessed by using six different values i.e., 3.0 mm, 2.5 mm, 2.0 mm, 1.5 mm, 1.0 mm, and 0.5 mm. By enhancing the t_{GFRP} from a minimum value of 0.5 mm to a maximum value of 3 mm along with enhancement of ρ_l from 1.2 to 2.2%, by keeping the contact values of $f'_{\text{co}} = 25$ MPa and $D = 200$ mm, an improvement of 64% occurred in the CS of FRCFS columns. Correspondingly, by enhancing the t_{GFRP} from a minimum value of 0.5 mm to a maximum value of 3 mm along with enhancement of D from 100 to 350 mm by keeping the contact values of $f'_{\text{co}} = 25$ MPa and $\rho_l = 1.8\%$, an improvement of 1050.9% occurred in the CS of FRCFS columns as reported in Fig. 10.

4.4 Diameter of Column (D)

The D was investigated for six levels: 350 mm, 300 mm, 250 mm, 200 mm, 150 mm, and 100 mm to examine its sensitivity on the axial compressive response of FRCFS columns. The result of the discrepancy of D is reported in Fig. 10(c, e, f). By enhancing the D from a minimum value of 100 mm to a maximum value of 350 mm along with enhancement of f'_{co} from 15 to 65 MPa by keeping the contact values of $t_{\text{GFRP}} = 2$ mm and $\rho_l = 1.8\%$, an improvement of 1282.7% occurred in the CS of FRCFS columns. Correspondingly, by enhancing the D from a minimum value of 100 mm to a maximum value of 350 mm along with enhancement of t_{GFRP} from 0.5 to 3 mm by keeping the contact values of $f'_{\text{co}} = 25$ MPa and $\rho_l = 1.8\%$, an improvement of 1051.7% occurred in the CS of FRCFS columns. Therefore, it can be concluded from the parametric study that the effect of enhancing ρ_l , f'_{co} , t_{GFRP} , and D of the FRCFS columns was important for the improvement in their ultimate CS.

5 Conclusions

In present work, two different large records for FRP-wrapping and FRP reinforcement were constructed from the previous research to apprehend the CS of FRCFS columns under axial loads. After evaluating the records using the previously recommended model, a new model was recommended for the axial CS of FRCFS columns. Following important points were extracted from the current study:

1. The performance of the suggested model for the CS of FRP-wrapped concrete specimens on the large previous experimental record of 500 specimens shows its superiority over the previous models. It represented a high

precision with $\text{RMSE} = 0.18$ and $R^2 = 0.91$ as compared with the previous models available in the literature.

2. The suggested theoretical model for the CS of GFRP-RC specimens represented better performance on the developed record of 269 specimens from the previous research with $R^2 = 0.73$ as compared with previous models available in the literature. The reduction coefficients for the CS of GFRP-RC compressive members due to concrete and FRP bars should be $0.85 - 0.0029f'_{\text{co}}$ and 0.0208 , respectively.
3. The parametric study using the suggested theoretical model investigated the influence of the enhancement of the thickness of the confining GFRP sheet, the internal longitudinal GFRP-reinforcement ratio, the diameter of columns, and the unwrapped concrete axial CS on the axial strength of GFRP-RC specimens.
4. The improvement in the axial ultimate capacity of FRCFS columns was observed by increasing all these parameters. By enhancing the reinforcement ratio from 1.2 to 2.2%, the CS was improved up to 212.5%; with the enhancement of GFRP sheet thickness from 0.5 to 3 mm, the CS was improved up to 64%; with the enhancement of CS of unwrapped concrete from 15 to 65 MPa, the CS was improved by 222.2%; and, lastly, with the enhancement of diameter of the column from 100 to 350 mm, and the CS was improved by 1282.7% that was the most dominant effect.

Acknowledgements None.

Compliance with Ethical Standards

Conflict of interest The authors declare that they have no conflicts of interest.

References

- AASHTO (2018) AASHTO LRFD bridge design guide specifications for GFRP-reinforced concrete
- Abdelazim W, Mohamed HM, Benmokrane B, Afifi MZ (2020a) Effect of critical test parameters on behavior of glass fiber-reinforced polymer-reinforced concrete slender columns under eccentric load. *ACI Struct J* 117(4):127–141
- Abdelazim W, Mohamed HM, Benmokrane B, Nolan S (2020b) Strength of bridge high-strength concrete slender compression members reinforced with GFRP bars and spirals: experiments and second-order analysis. *J Bridge Eng* 25(9):04020066
- ACI (2011a) Building code requirements for structural concrete and commentary. UACI, Farmington Hills, pp 318–411
- ACI (2002) Guide for the design and construction of externally bonded FRP systems for strengthening concrete structures. 440
- ACI Committee 318–11 (2011b) American concrete institute. Farmington Hills, MI, p 473



- Afifi MZ, Mohamed HM, Benmokrane B (2013a) Axial capacity of circular concrete columns reinforced with GFRP bars and spirals. *J Compos Constr* 18(1):04013017
- Afifi MZ, Mohamed HM, Benmokrane B (2013b) Strength and axial behavior of circular concrete columns reinforced with CFRP bars and spirals. *J Compos Constr* 18(2):04013035
- Afifi MZ, Mohamed HM, Chaallal O, Benmokrane B (2014) Confinement model for concrete columns internally confined with carbon FRP spirals and hoops. *J Struct Eng* 141(9):04014219
- Al-Nimry H, Neqresh M (2019) Confinement effects of unidirectional CFRP sheets on axial and bending capacities of square RC columns. *Eng Struct* 196:109329
- Bagheri M, Chahkandi A, Jahangir H (2019) Seismic reliability analysis of RC frames rehabilitated by glass fiber-reinforced polymers. *Int J Civ Eng* 17(11):1785–1797
- Canadian Standards Association (2012a) Canadian standards association, Mississauga, ON, Canada, 177 pp. 48
- Canadian Standards Association (2019) Canadian highway bridge design code (CAN/CSA S6-19). Toronto, Ontario
- Canadian Standards Association (CSA) (2012b) Design and construction of building components with fiber reinforced polymers. CAN/CSAS806–12
- Dadvar SA, Mostofinejad D, Bahmani H (2020) Strengthening of RC columns by ultra-high performance fiber reinforced concrete (UHPC) jacketing. *Constr Build Mater* 235:117485
- De Luca A, Matta F, Nanni A (2010) Behavior of full-scale glass fiber-reinforced polymer reinforced concrete columns under axial load. *ACI Struct J* 107(5):589
- Dong M, Elchalakani M, Karrech A, Pham TM, Yang B (2019) Glass fibre-reinforced polymer circular alkali-activated fly ash/slag concrete members under combined loading. *Eng Struct* 199:109598
- Elchalakani M, Dong M, Karrech A, Li G, Mohamed Ali MS, Yang B (2019) Experimental investigation of rectangular air-cured geopolymer concrete columns reinforced with GFRP bars and stirrups. *J Compos Constr* 23(3):04019011
- Elchalakani M, Ma G (2017) Tests of glass fibre reinforced polymer rectangular concrete columns subjected to concentric and eccentric axial loading. *Eng Struct* 151:93–104
- Elchalakani M, Ma G, Aslani F, Duan W (2017) Design of GFRP-reinforced rectangular concrete columns under eccentric axial loading. *Mag Concr Res* 69(17):865–877
- Elmessalami N, Refai AE, Abed F (2019) Fiber-reinforced polymers bars for compression reinforcement: a promising alternative to steel bars. *Constr Build Mater* 209:725–737
- Elshamandy MG, Farghaly AS, Benmokrane B (2018) Experimental behavior of glass fiber-reinforced polymer-reinforced concrete columns under lateral cyclic load. *ACI Struct J* 115(2):337–349
- Fardis MN, Khalili HH (1982) FRP-encased concrete as a structural material. *Mag Concr Res* 34(121):191–202
- Hadhood A, Mohamed HM, Benmokrane B (2016) Axial load–moment interaction diagram of circular concrete columns reinforced with CFRP bars and spirals: experimental and theoretical investigations. *J Compos Constr* 21(2):04016092
- Hadhood A, Mohamed HM, Benmokrane B, Nanni A, Shield CK (2019) Assessment of design guidelines of concrete columns reinforced with glass fiber-reinforced polymer bars. *ACI Struct J* 116(4):193–207
- Hadi MN, Khan QS, Sheikh MN (2016) Axial and flexural behavior of unreinforced and FRP bar reinforced circular concrete filled FRP tube columns. *Constr Build Mater* 122:43–53
- Hasan HA, Sheikh MN, Hadi MN (2019) Maximum axial load carrying capacity of fibre reinforced-polymer (FRP) bar reinforced concrete columns under axial compression. *Structures* 19:227–233
- Hassan A, Khairallah F, Mamdouh H, Kamal M (2018) Evaluation of self-compacting concrete columns reinforced with steel and FRP bars with different strengthening techniques. *Structures* 15:82–93
- Hosseini SM, Mostofinejad D, Saljoughian A, Nader Tehrani B (2020) Seismic retrofit of square RC short columns with shear-flexural failure mode via CFRP composites using different confinement techniques. *J Compos Constr* 24(4):04020029
- Karbhari VM, Gao Y (1997) Composite jacketed concrete under uniaxial compression—Verification of simple design equations. *J Mater Civ Eng* 9(4):185–193
- Karim H, Sheikh MN, Hadi MNS (2016) Axial load-axial deformation behaviour of circular concrete columns reinforced with GFRP bars and helices. *Constr Build Mater* 112:1147–1157
- Khan QS, Sheikh MN, Hadi MNS (2016) Axial-flexural interactions of GFRP-CFFT columns with and without reinforcing GFRP bars. *J Compos Constr* 21(3):04016109
- Khorramian K, Sadeghian P (2017) Experimental and analytical behavior of short concrete columns reinforced with GFRP bars under eccentric loading. *Eng Struct* 151:761–773
- Lam L, Teng JG (2003) Design-oriented stress–strain model for FRP-confined concrete. *Constr Build Mater* 17(6–7):471–489
- Lim JC, Karakus M, Ozbakkaloglu T (2016) Evaluation of ultimate conditions of FRP-confined concrete columns using genetic programming. *Comput Struct* 162:28–37
- Lim JC, Ozbakkaloglu T (2014) Confinement model for FRP-confined high-strength concrete. *J Compos Constr* 18(4):04013058
- Mai AD, Sheikh MN, Hadi MN (2018) Influence of the location of CFRP strips on the behaviour of partially wrapped square reinforced concrete columns under axial compression. *Structures* 15:131–137
- Mai AD, Sheikh MN, Yamakado K, Hadi MN (2020) Nonuniform CFRP wrapping to prevent sudden failure of FRP confined square RC columns. *J Compos Constr* 24(6):04020063
- Mander JB, Priestley MJ, Park R (1988) Theoretical stress-strain model for confined concrete. *J Struct Eng* 114(8):1804–1826
- Matthys S, Toutanji H, Audenaert K, Taerwe L (2005) Axial load behavior of large-scale columns confined with fiber-reinforced polymer composites. *ACI Struct J* 102(2):258
- Miyauchi K (1997) Estimation of strengthening effects with carbon fiber sheet for concrete column. In Proceedings of the 3rd international symposium on non-metallic (FRP) reinforcement for concrete structures. Japan concrete institute
- Mohamed H, Afifi MZ, Benmokrane B (2014a) Performance evaluation of concrete columns reinforced longitudinally with FRP bars and confined with FRP hoops and spirals under axial load. *J Bridge Eng* 19(7):04014020
- Mohamed HM, Benmokrane B (2013) Design and performance of reinforced concrete water chlorination tank totally reinforced with GFRP bars: case study. *J Compos Constr* 18(1):05013001
- Mohamed HM, Benmokrane B (2016) Reinforced concrete beams with and without FRP web reinforcement under pure torsion. *J Bridge Eng* 21(3):04015070
- Mohamed HM, Chaallal O, Benmokrane B (2014b) Torsional moment capacity and failure mode mechanisms of concrete beams reinforced with carbon FRP bars and stirrups. *J Compos Constr* 19(2):04014049
- Moshiri N, Hosseini A, Mostofinejad D (2015) Strengthening of RC columns by longitudinal CFRP sheets: effect of strengthening technique. *Constr Build Mater* 79:318–325
- Mostofinejad D, Ilia E (2014) Confining of square RC columns with FRP sheets using corner strip-batten technique. *Constr Build Mater* 70:269–278
- Mostofinejad D, Moshiri N (2015) Compressive strength of CFRP composites used for strengthening of RC columns: comparative evaluation of EBR and Grooving Methods. *J Compos Constr* 19(5):04014079
- Mostofinejad D, Torabian A (2016) Experimental study of circular RC columns strengthened with longitudinal CFRP composites

- under eccentric loading: comparative evaluation of EBR and EBRG methods. *J Compos Constr* 20(2):04015055
- Naderpour H, Mirrashid M (2020) Confinement coefficient predictive modeling of FRP-confined RC columns. *Adv Civ Eng Mater* 9(1):1–21
- Newman K, Newman JB (1971) Failure theories and design criteria for plain concrete. *Struct Solid Mech Eng Design* 36:963–995
- Pantelides CP, Gibbons ME, Reaveley LD (2013) Axial load behavior of concrete columns confined with GFRP spirals. *J Compos Constr* 17(3):305–313
- Rasouli M, Broujerdian V, Kazemzadeh A (2020) Predicting the compressive stress-strain curve of FRP-confined concrete column considering the variation of Poisson's ratio. *Int J Civ Eng* 18:1–16
- Raza A, Ali B, Rehman A (2020a) Structural performance of steel-tube concrete columns confined with CFRPs: numerical and theoretical study. *Iran J S Technol Trans Civ Eng* 1–18
- Raza A, Khan QUZ, Ahmad A (2020b) Investigation of HFRC columns reinforced with GFRP bars and spirals under concentric and eccentric loadings. *Eng Struct* 227:111461
- Raza A, Khan QuZ, Ahmad A (2020c) Reliability analysis of proposed capacity equation for predicting the behavior of steel-tube concrete columns confined with CFRP sheets. *Comput Concr* 25(5):383–400
- Raza A, Khan QUZ, Ahmad A (2020d) Prediction of axial compressive strength for FRP-Confined concrete compression members. *KSCE J Civ Eng* 24(7):2099–2109
- Raza A, Rafique U (2020) Efficiency of GFRP bars and hoops in recycled aggregate concrete columns: experimental and numerical study. *Compos Struct* 255:112986
- Richart FE, Brandtæg A, and Brown RL (1929) Failure of plain and spirally reinforced concrete in compression. University of Illinois at Urbana Champaign, College of Engineering
- Saafi M, Toutanji H, Li Z (1999) Behavior of concrete columns confined with fiber reinforced polymer tubes. *Mater J* 96(4):500–509
- Sadeghian P, Fam A (2015) Improved design-oriented confinement models for FRP-wrapped concrete cylinders based on statistical analyses. *Eng Struct* 87:162–182
- Saljoughian A, Mostofinejad D, Hosseini SM (2019) CFRP confinement in retrofitted RC columns via CSB technique under reversed lateral cyclic loading. *Mater Struct* 52(4):67
- Saljoughian A, Mostofinejad D (2017) Rectangular reinforced concrete columns strengthened with carbon fiber-reinforced polymer sheets using corner stripbatten method. *ACI Struct J* 114(3):659–671
- Samaan M, Mirmiran A, Shahawy M (1998) Model of concrete confined by fiber composites. *J Struct Eng* 124(9):1025–1031
- Samani AK, Attard MMA (2012) Stress-strain model for uniaxial and confined concrete under compression. *Eng Struct* 41:335–349
- Tabatabaei A, Eslami A, Mohamed HM, Benmokrane B (2018) Strength of compression lap-spliced GFRP bars in concrete columns with different splice lengths. *Constr Build Mater* 182:657–669
- Tabatabaei A, Mohamed HM, Eslami A, Benmokrane B (2020) Proposed design equations for lap splice of glass fiber-reinforced polymer bars under compression in concrete. *ACI Struct J* 117(2):291–302
- Teng JG, Jiang T, Lam L, Luo YZ (2009) Refinement of a design-oriented stress-strain model for FRP-confined concrete. *J Compos Constr* 13(4):269–278
- Tobbi H, Farghaly AS, Benmokrane B (2012) Concrete columns reinforced longitudinally and transversally with glass fiber-reinforced polymer bars. *ACI Struct J* 109(4):551–558
- Tobbi H, Farghaly AS, Benmokrane B (2014) Behavior of concentrically loaded fiber-reinforced polymer reinforced concrete columns with varying reinforcement types and ratios. *ACI Struct J* 111(2):375–386
- Tošić N, de la Fuente A, Marinković S (2018) Shrinkage of recycled aggregate concrete: experimental database and application of fib Model Code 2010. *Mater Struct* 51(5):126
- Toutanji H (1999) Stress-strain characteristics of concrete columns externally confined with advanced fiber composite sheets. *Mater J* 96(3):397–404
- Van Cao V, Pham SQ (2019) Comparison of CFRP and GFRP wraps on reducing seismic damage of deficient reinforced concrete structures. *Int J Civ Eng* 17(11):1667–1681
- Xue W, Hu X, Fang Z (2014) Experimental studies of GFRP reinforced concrete columns under static eccentric loading. In 7th international conference on fiber reinforced polymer (FRP) composites in civil engineering (CICE 2014), International institute for FRP in construction (IIFC), Kingston, ON, Canada
- Zadeh HJ, Nanni A (2012) Design of RC columns using glass FRP reinforcement. *J Compos Constr* 17(3):294–304